On the visco-elastic properties of open-cell polyurethane foams

Gianpietro del Piero, Giampiero Pampolini

On the visco-elastic properties of open-cell polyurethane foams in uniaxial compression

Gianpietro DEL PIERO[*], Giampiero PAMPOLINI[*#]

[*]*Università di Ferrara, Via Saragat 1, 44100 Ferrara, Italy*
E-mail: dlpgpt@unife.it

[#]*LMA, C.N.R.S., 31 chemin Joseph Aiguier, 13402 Marseille, France*
E-mail: pampolini@lma.cnrs-mrs.fr

Abstract. This communication is a summary of our previous work [12] on the elastic properties of open-cell polyurethane foams, and an anticipation of some results of a work in progress [2] on the rate-dependent properties of the same material. The elastic properties are described by a two-phase model obtained assuming a non-convex double-well strain energy density. The model captures some peculiar aspects of the stress-strain response of the material, such as strain localization and hysteresis. But it does not capture some typical inelastic effects, such as stress softening in a cyclic test, rate dependence, and memory effects. On the basis of some specific compression tests, we come to the conclusion that these effects can be described within the theory of linear viscoelasticity. This leads us to complete the previous elastic model by adding a visco-elastic element with fractional damping.

1 Introduction

Polymeric open-cell foams have a complex non-linear behavior. In uniaxial compression, the response curve exhibits three well distinguishable regimes: an initial ascending branch, a large plateau, and a second ascending branch. At unloading, instead of following backwards the loading path, the response exhibits a hysteresis loop. Moreover, while in the ascending branches the foam deforms homogeneously, in the plateau regime a localization of deformation takes place on layers orthogonal to the loading direction [6, 12, 14].

In the literature, many studies, mostly based on numerical simulations, have been addressed to the relationship between microstructure and elastic properties [3, 4, 6]. Usually, the foam is represented as a periodic structure made of linear elastic beams, and strain localization is attributed to the buckling of the cell ligaments [6]. In the model proposed in [12], strain localization is instead attributed to a special non-convex shape of the strain energy density, which is also responsible of the hysteresis loops observed in cyclic tests. The model is in a good qualitative agreement with the experiments. There are, however, some aspects of the observed response which cannot be reproduced by a purely elastic model. Specifically, they are:

- *Stress softening*, that is, a progressive reduction of the stress with increasing number of cycles in a cyclic test, Fig. 2a,
- *Rate dependence*, revealed by an apparent increase of strength with increasing loading rate, Fig. 3,
- *Memory effect*, consisting of a partial recovering of strength at sufficiently delayed reloading, Fig. 2d.

The phenomenon of stress softening is also observed in filled rubbery polymers, for which it is known as the *Mullins effect* [7, 10, 11]. This effect is generally attributed to the interactions between the polymeric matrix and the fillers, and is sometimes regarded as a form of isotropic damage [1, 9]. For polymeric foams, the recovery in time of the loading curves, Fig. 2d, rather suggests that this phenomenon be due to a memory effect.

This communication contains a summary of our preceding paper [12] on the elastic model, and an anticipation of our new model which accounts for the inelastic effects listed before, and which will be fully described in the forthcoming paper [2].

2 Experiments

The experiments described below were made on a load frame Instron 4467 with a 500 N load cell, located at the *Laboratorio di Materiali Polimerici* of the University of Ferrara. The specimens were parallelepipeds with base dimensions 100 x 100 mm, cut out from a 50 mm thick sheet of commercial open-cell polyurethane foam. The cutting was done manually, using a ribbon saw. A pre-load of 2 to 3 N was applied to guarantee a full initial contact between plate and specimen. All tests were made at room temperature, controlling the displacement of the upper crosshead, and measuring the force exerted by the sample.

In all following figures, the *stress* is the force divided by the initial area, and the *deformation* is the ratio between the displacement of the upper crosshead and the initial distance between the upper crosshead and the basis.

2.1 Strain localization

To get evidence of strain localization, we performed a uniaxial compression test, with a rectangular grid drawn on one of the specimens' sides. The progressive deformation of the grid under a crosshead displacement growing with a speed of 5 mm/min, is shown in Fig. 1. After an initial regime of homogeneous deformation, Fig. 1a, a severe deformation occurred at the specimen's ends, Fig. 1b. This deformation then propagated towards the central layers, Fig. 1c and 1d, and finally, after all layers had been reached, the deformation again became homogeneous, Fig. 1e.

2.2 Cyclic compression tests

Cyclic compression tests were performed on three samples, at a crosshead speed of 5 mm/min. The direction of motion of the crosshead was reversed when the displacement reached the value of 35 mm, and reversed again at complete unloading, when the load cell measured a null force. Each sample was subjected to four series of four cycles, separated by three resting periods of the duration of 16 hours, 52 hours, and 33 days, respectively. In Fig. 2 the average stress-deformation curves of the three samples are reported. In the loading curves, there is a sharp stress reduction between the first and the second cycle, and a more modest reduction in the subsequent cycles. At unloading, the response curves are almost the same for all cycles.

By comparing Figures 2a and 2b, we see that after a resting period of 16 hours there is a complete recovery of the strength lost in the last two cycles of the first series. From the following figures we see that there are no significant changes after 52 hours, while

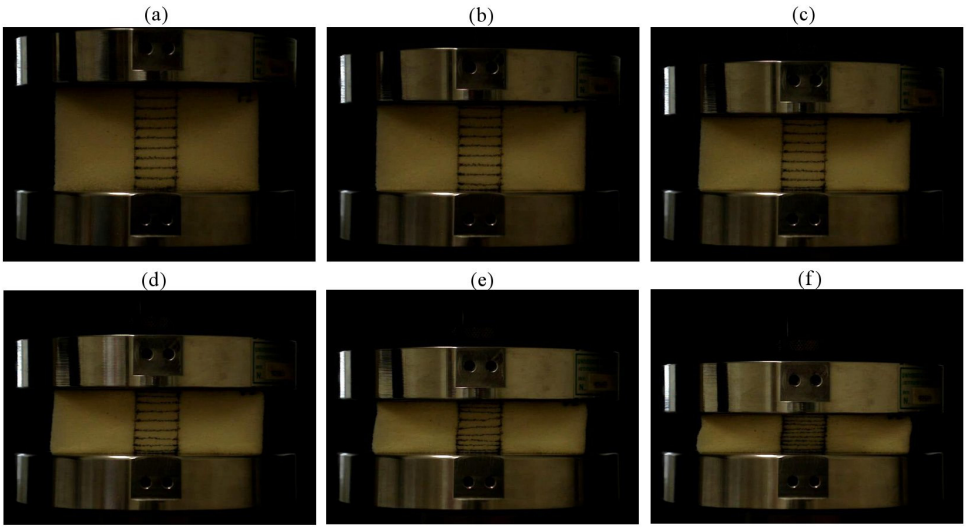

Figure 1. The progressive localization mechanism: the initial homogeneous deformation (a), the first strain localization at the specimen's ends (b), the subsequent propagation to the central layers (c), (d), (e), and the new homogeneous deformation (f).

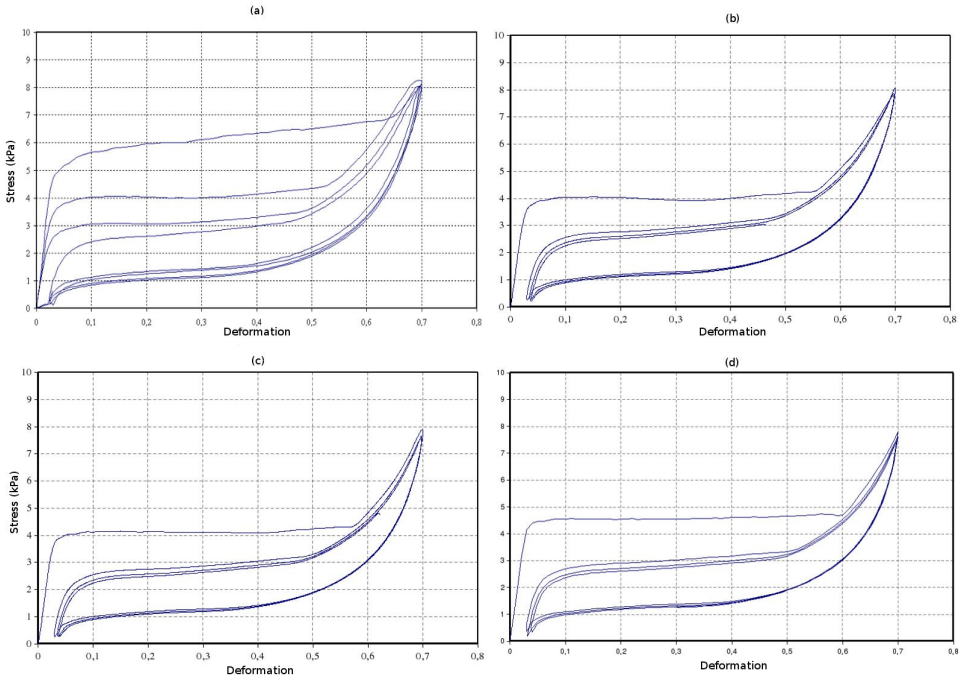

Figure 2. Force-elongation curves for cyclic compression in a virgin specimen (a), and after a resting period of 16 hours (b), 52 hours (c), and 33 days (d). Crosshead speed of 5 mm/min.

after 33 days there is a stepping up of the loading curve of the first cycle, with an increase from 4 to almost 4.5 kPa. Thus, there is a slow recovery of the strength lost in the first series of cycles.

Finally, to get evidence of the rate-dependence of the response we made some cyclic compression tests at the constant crosshead speeds of 0.1, 5, and 100 mm/min. Three samples were tested for each velocity. The average force-elongation curves shown in Figure 3 reveal an overall lifting of the response curves at increasing velocity.

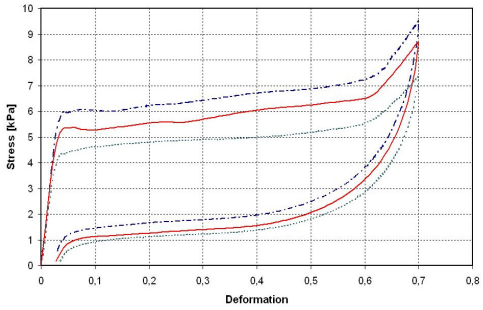

Figure 3. Stress-deformation curves in cyclic tests made at different velocities: 0.1 mm/min (dotted line), 5 mm/min (full line) and 100 mm/min (dashed line)

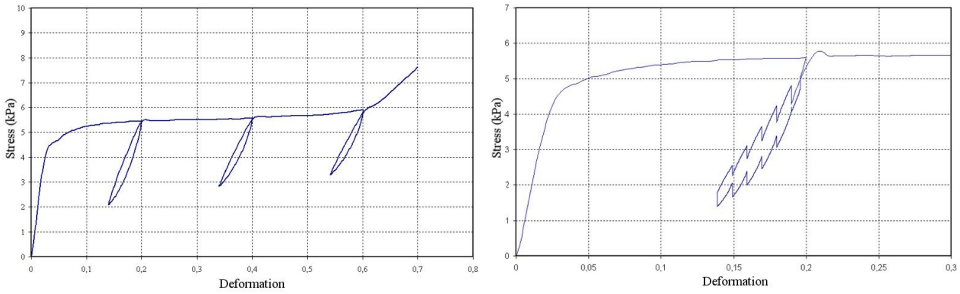

Figure 4. Loading-unloading cycles with small amplitudes starting from the upper plateau, without interruption (left), and with rest intervals of 45 minutes (right).

2.3 Relaxation tests

With the goal of investigating the elastic character of the loading-unloading curves, we performed some small-amplitude loading-unloading cycles, starting from three different points in the upper plateau, Fig. 4a. The observed small hysteresis loops suggest the presence of viscous phenomena. This presence is made evident by the next test, Fig. 4b, in which a similar cycle was interrupted several times, with rest intervals of 45 minutes. The vertical segments in correspondence of the rest intervals denote the presence of stress relaxation.

We then proceeded to the determination of the relaxation function. For this purpose, relaxation tests were performed on three samples. They were compressed at a crosshead speed of 250 mm/min, till the crosshead displacement reached 35 mm. At this point, the upper crosshead was blocked and held in position for 72 hours, measuring the force at

intervals of 1 minute. The average stress-time curve is given in Fig. 5. It shows a very fast relaxation in the first few minutes, and a much slower relaxation afterwards.

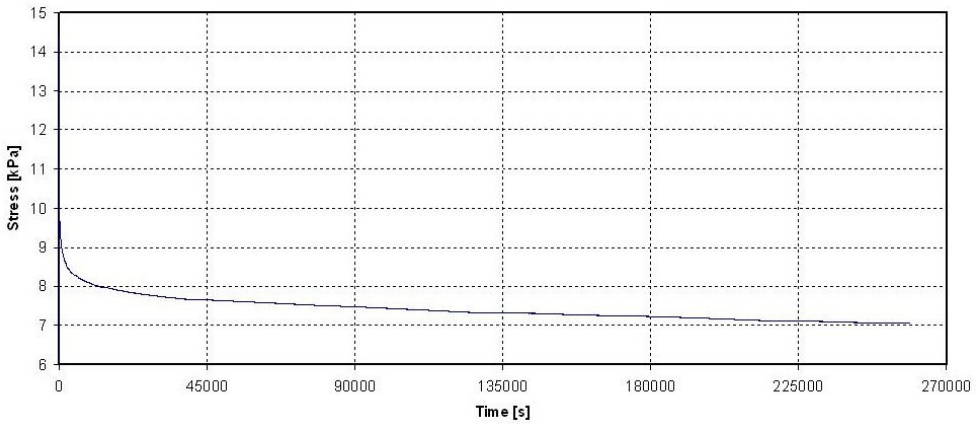

Figure 5. Stress-time curve of the 72-hours relaxation test.

3 The theoretical model

3.1 The chain of springs

In the elastic model proposed in [12], the foam is represented as a chain of non-linear elastic springs with non-convex strain energy. We suppose that the specimen is made of cells, Fig. 6a, and that each layer of cells is represented by a non-linear elastic spring, Fig. 6b. We also assume that all springs have the same energy w, and that this energy only depends on the elongation ε of the spring. The non-convex form assumed for w is shown in Fig. 6c. The corresponding stress-strain curve has two ascending branches separated by a descending branch, as shown in Fig. 6d. The two ascending branches form the phase A and the phase B of the material, respectively. The equilibrium configurations of the chain are identified with the local minimizers of the total energy

$$E(\varepsilon_1, \ldots \varepsilon_n) = \sum_{i=1}^{n} w(\varepsilon_i)\,, \tag{1}$$

subjected to the *hard device* condition

$$\sum_{i=1}^{n} \varepsilon_i = n\varepsilon_0\ , \qquad i = 1,2,\ldots n, \tag{2}$$

where $n\varepsilon_0$ is the given displacement of the upper basis, the displacement at the lower basis being zero.

From the condition of stationarity of the energy it follows that the forces transmitted across the springs all have the same value, which we denote by σ [12]. Moreover, for sufficiently large n, a necessary condition for an energy minimum is that all elongations ε_i lie on one of the two ascending branches of the stress-strain curve, see [12] for details. Accordingly, a local minimizer may have m springs in the phase A and $n-m$ springs in the phase B, with m any number between 0 and n. The local energy minimizers form

metastable equilibrium paths in the configuration space. In Fig. 7a, the projections of these paths in the (σ,ε_0) plane are shown for a chain made of four springs. If one assumes that the system evolves along metastable equilibrium paths, then the system, when loaded starting from the configuration $\varepsilon_i = 0$, initially follows the first ascending branch. This branch ends when σ reaches the value σ^{max}. At this point, for further increasing deformation it is reasonable to assume that the system jumps to the closest stable branch, corresponding to the configuration with one spring in phase B and three springs in phase A. When this branch ends, the system jumps to the branch with two springs in phase B and so on, until all springs undergo the phase transition. At this point the system evolves following the second ascending branch, which corresponds to single-phase configurations with all springs in phase B.

If we now increase the number of the springs, the number of the intermediate branches increases, and the amplitudes of the jumps at the end of the branches decrease, Fig. 7b. In this case, after reaching the critical value σ^{max}, the system follows a wavy, approximately horizontal line. The same occurs at unloading, after reaching the critical value σ^{min}.

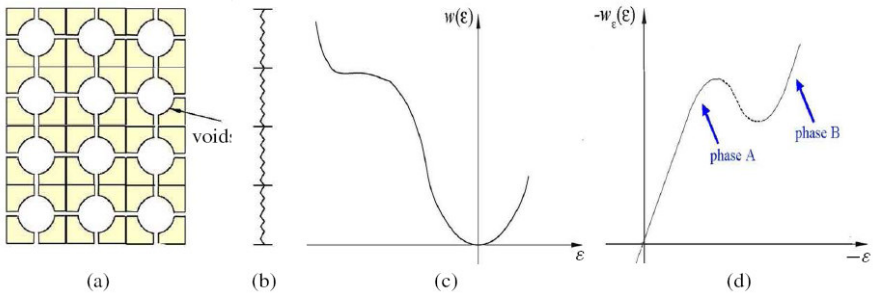

Figure 6. Subdivision of the body into cell layers (a), and representation of each layer as a non-linear elastic spring (b). The non convex shape assumed for the energy of a spring (c), and the corresponding non-monotonic stress-strain curve (d).

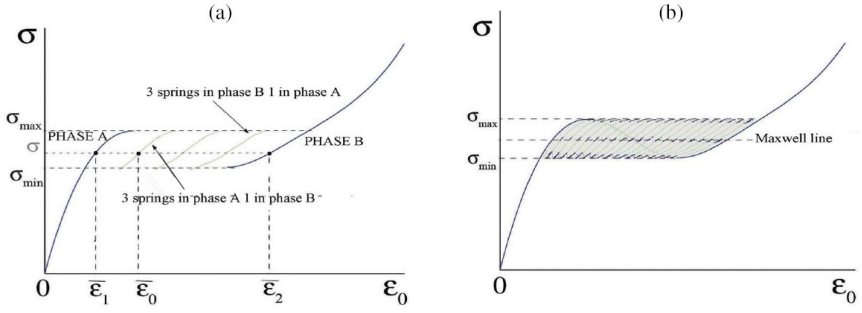

Figure 7. Response curves for a system of four springs (a), and for a system of twenty springs (b).

3.2 *The dashpot*

For the dashpot we assume a linear viscoelastic law of the Boltzmann-Volterra type

$$\sigma(t) = \int_{-\infty}^{t} G(t-s)\dot{\varepsilon}(s)ds\,, \tag{3}$$

where G is the relaxation function, t is the time, and the dot denotes time differentiation. For the relaxation function we assume the power law

$$G(t) = \frac{k}{\Gamma(1-\alpha)} t^{-\alpha}\,, \tag{4}$$

where Γ is the Gamma function, k is a positive constant, and $0 < \alpha \leq 1$. This function corresponds to the damping element, called 'spring-pot' by Koeller [5], and governed by the fractional law

$$\sigma(t) = k \frac{\partial^{\alpha}}{\partial t^{\alpha}} \varepsilon(t)\,. \tag{5}$$

which reduces to $\sigma = k\dot{\varepsilon}$ if $\alpha = 1$, for details see [8]. The choice of this law is motivated by the shape of the relaxation function revealed by the experiments, see Figures 3 and 5. Indeed, power laws relaxation functions are appropriate to describe a very quick relaxation, followed by a much slower relaxation of long duration, see [5, 8].

3.3 *The visco-elastic model*

The visco-elastic model consists of a chain whose elements are composed of a spring and a dashpot connected in parallel. Let us denote by ε_i the elongation of the i-th element. The system is still subjected to the hard device condition (2), and the force σ is still the same for all elements. This force is now the sum of two contributions: an elastic term due to the spring, and a dissipative term due to the dashpot:

$$\sigma(t) = w'(\varepsilon_i) + \int_{0}^{t} G(t-s)\dot{\varepsilon}_i(s)ds\,, \quad i = 1, 2, \ldots, N\,. \tag{6}$$

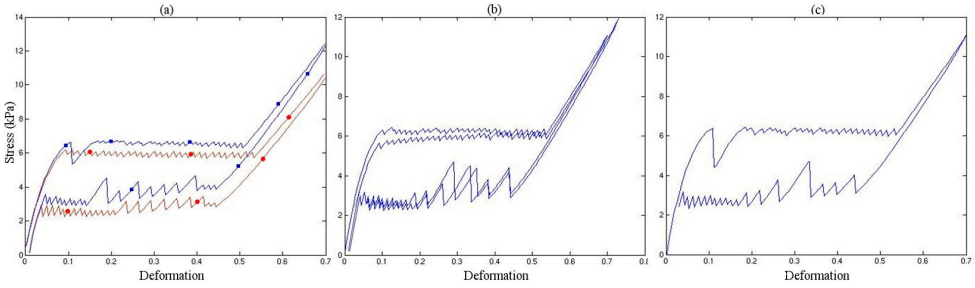

Figure 8. Response curves for a system of 30 elements: two loading-unloading tests at two different strain rates, 5 mm/min (round markers) and 100 mm/min (square markers) (a), a cyclic compression test (b), and a loading-unloading test including a resting period of 72 hours (c).

To find the response of the system some numerical experiments are in progress. Only preliminary results are available at this stage. More complete results will be presented in the forthcoming paper [2].

The curves in Figure 8 are relative to a system of 30 elements subject to three different loading-unloading processes: single loading-unloading tests at different strain rates, Fig. 8a, a cyclic test, Fig. 8b, and a loading-unloading test including a resting period of 72 hours, Fig. 8c. These results show that the three phenomenological aspects mentioned in the Introduction are all captured by the proposed model. In particular, the model exhibits:

- an increase of the force with increasing load rate in both loading and unloading curves, Fig. 3 and 8a,
- a drop of the loading curve and a more gradual transition from the first ascending branch to the plateau at the second cycle of the cyclic test, Fig. 8b,
- the independence of the unloading curves on the number of cycles, Fig. 8b,
- a residual deformation after a loading-unloading process, Fig. 8a and 8b,
- a partial stress recovery after a resting period of 72 hours, Fig. 8c.

References

[1] M.F. Beatty, S. Krishnaswamy. A theory of stress-softening in incompressible isotropic materials. *J. Mech. Phys. Solids* **48**: 1931–1965, 2000.

[2] G. Del Piero, G. Pampolini. The inelastic properties of open-cell polymeric foams: experiments and theoretical model, *in preparation.*

[3] L. J. Gibson, M.F. Ashby. *Cellular Solids: Structure and Properties*. Cambridge University Press, second edition, 1997.

[4] L. Gong, S. Kyriakides. On the crushing stress of open cell foams. *J. Appl. Mech.* **73**: 807-814, 2007.

[5] R.C. Koeller. Applications of Fractional Calculus to the Theory of Viscoelasticity, *J. Appl. Mech.* **51**: 299–307, 1984.

[6] R. Lakes, P. Rosakis, and A. Ruina. Microbuckling instability in elastomeric cellular solids. *J. Mater. Sci.* **28**: 4667-4672, 1993.

[7] A, Lion, A constitutive model for carbon black filled rubber. Experimental investigations and mathematical representations. *Cont. Mech. Thermodyn*. **8**: 153–169 1996.

[8] A. Lion. On the thermodynamics of fractional damping elements, *Cont. Mech. Thermodyn*. **9**: 83–96, 1997.

[9] C. Miehe, J. Keck, Superimposed finite elastic-viscoelastic-plastoelastic stress response with damage in filled rubbery polymers. Experiments, modelling and algorithmic implementation. *J. Mech. Phys. Solids* **48**: 323–365, 2000.

[10] L. Mullins, Softening of rubber by deformation. *Rubber Chem. Technol*. **42**, 339–362, 1969.

[11] L. Mullins, N.R. Tobin, Theoretical model for the elastic behavior of filler-reinforced vulcanized rubbers. *Rubber Chem. Technol*. **30**: 555–571, 1957.

[12] G. Pampolini, G. Del Piero. Strain localization in open-cell polyurethane foams: experiments and theoretical model. *J. Mech. of Materials and Structures*, **3**: 969-981, 2008.

[13] G. Puglisi, L. Truskinovsky. Mechanics of a discrete chain with bi-stable elements. *J. Mech. Phys. Solids* **48**: 1-27, 2000.

[14] Y. Wang, A.M. Cuitinho. Full-field measurements of heterogeneous deformation patterns on polymeric foams using digital image correlation. *Int. J. Solids Structures* **39**: 3777-3796, 2002.